International Journal of Pavement Engineering
Publication details, including instructions for authors and subscription information:
http://www.tandfonline.com/loi/gpav20

Laboratory simulation tests of effect of mechanical damage on moisture damage evolution in hot-mix asphalt pavement

Xinzhuang Cui[a], Jiong Zhang[a], Na Zhang[a], Yaxu Zhou[a], Zhijun Gao[a] & Wei Sui[a]
[a] School of Civil Engineering, Shandong University, No. 17922 Jingshi Road, Jinan 250061, P.R. China
Published online: 07 Aug 2014.

International Journal of Pavement Engineering, 2014
http://dx.doi.org/10.1080/10298436.2014.943221

Laboratory simulation tests of effect of mechanical damage on moisture damage evolution in hot-mix asphalt pavement

Xinzhuang Cui, Jiong Zhang*, Na Zhang, Yaxu Zhou, Zhijun Gao and Wei Sui

School of Civil Engineering, Shandong University, No. 17922 Jingshi Road, Jinan 250061, P.R. China

(*Received 3 July 2013; accepted 5 July 2014*)

Moisture damage of hot-mix asphalt (HMA) pavement is an extremely complicated mode of distress. Previous researches on moisture damage mainly focused on the performances of undamaged pavement at the initial stage of opening to traffic. So with the permeability tests and the Hamburg Wheel Tracking Device (HWTD) tests, trial works were done to study the effect of traffic-load-induced mechanical damage on the evolution of moisture damage in HMA pavement. The monotonous uniaxial compression loading method and the repetitive compression loading method were employed to make the mechanical damages of the styrene–butadiene–styrene block copolymer-modified HMA specimens, respectively. Comparisons demonstrated that there were slight differences between the damages from the two kinds of damage making methods. The damages were characterised with two kinds of nondestructive testing methods (dynamic modulus testing method and ultrasonic wave testing method), and the relationship of the characterised damages with the two methods was obtained. The permeability tests of HMA showed that the coefficient of permeability initially decreases and then increases with the damage. HWTD test results implied that the mechanical damage had a significant influence on the moisture damage, especially in hot and humid environment. In HWTD test, the mechanical damage induced by the undesirable stress state in pavement accelerates the appearance of the striping inflection point and increases the cumulative deformation of HMA specimen. Therefore, in order to reflect the performance of asphalt pavement during its life cycle, the effect of mechanical damage on the evolution of moisture damage should be considered in pavement design and construction.

Keywords: HMA pavement; moisture damage; mechanical damage; permeability; water stability

1. Introduction

In recent years, transportation has attained prominent achievements in China. The total expressway length was about 100,000 km and had already ranked first in the world by the end of 2012. With the rapid development of the expressway, it has been paid more and more attention to pavement distresses. Some surveys indicate after opening to traffic for one or two years, many expressways with hot-mix asphalt (HMA) pavement have serious distresses such as rutting, shoving, ravelling or cracking and so on. These early pavement distresses induced by water are collectively called moisture damage. Moisture damage is recognised as a major issue, resulting to the need for frequent maintenance operations. This does not only imply high maintenance costs, but also increases traffic congestion. Given the high costs for the road authorities and the inconvenience for the users, it is greatly desired to shift the solution from a repair philosophy to a prevention one.

In the pavement design, the permeability of HMA mixture is a key parameter related to moisture damage. Krishnan and Bao (2001) found that the permeability has an exponential function with the air voids. Terrel and Al-Swailini (1993) investigated empirical relations between permeability and air voids. According to the investigation, for air voids less than 5%, the mixture is termed as impermeable; for air voids more than 15%, the mixture is considered free draining or totally permeable; and for air voids in the range from 5 to 15%, the mixture is considered to be in the pessimum voids range. However, Brown (1990) found that for air voids less than 8%, the permeability was not considered as a problem to cause moisture damage.

Another factor affecting moisture damage in HMA pavement is water stability of HMA mixture. A large number of studies have been conducted on water stability in terms of influencing factors (Airey *et al.* 2008, Guo *et al.* 2011), experimental methods (Solaimanian *et al.* 1993, Cheng *et al.* 2002, Hicks *et al.* 2003, Masad *et al.* 2006, Delaporte *et al.* 2008, Kanitpong and Pummarin 2010), evaluation indicators (Al-Swailmi and Terrel 1992, Aschenbrener 1995, Buchanan and Moore 2005), improvement measures (Mohammad *et al.* 2000, Kanitpong and Bahia 2005, Yuan *et al.* 2011) and moisture damage mechanism and so on. Studies done by Kringos and Scarpas (2008), Terrel and Al-Swailmi (1994), Kiggundu and Roberts (1988) and Taylor and Khosla (1983) revealed at least five different mechanisms of stripping: detachment, displacement, spontaneous emulsification, pore pressure and hydraulic scour. Cui (2010) developed dynamic water pressure sensor that can be laid in the HMA pavement during the high-temperature paving

*Corresponding author. Email: jiongzhang@sdu.edu.cn

process, and the sensor was used to capture the time history of the development and dissipation of traffic-load-induced pore water pressure.

Moisture damage is an extremely complicated mode of distress. Previous researches (Cui 2010, Yuan *et al.* 2011) on permeability and water stability of HMA mixture are mainly focused on the performance of undamaged specimens and reflect materials performance in the early stage of opening to traffic. However, numerous field investigations revealed that in the running process of road, the development of mechanical damage in pavement induced by repeated traffic loads can significantly influence the evolution of moisture damage. Although many studies (Cui 2010, Yuan *et al.* 2011) have been done about the moisture damage induced by the loss of stiffness and structural strength of pavement, the effect of mechanical damage (such as cracking) on the evolution of moisture damage has not been studied.

In this paper, a preliminary study was performed on the effect of mechanical damage on moisture damage based on laboratory simulation tests. Damages of styrene–butadiene–styrene block copolymer (SBS)-modified asphalt mixture specimens were made with the monotonous load method and the repetitive load method, and characterised with the dynamic modulus method and the ultrasonic wave method, respectively. Permeability tests and Hamburg Wheel Tracking Device (HWTD) tests were carried out to investigate the effect of mechanical damage on moisture damage evolution.

2. Test materials

In the test, SBS-modified asphalt is used as the binder of HMA. SBS is a kind of modified asphalt agent widely used in China, which has a better resilience feature, high-temperature stability and low-temperature anti-cracking performance. The basic property indexes of SBS-modified asphalt obtained according to Chinese specification of Standard Test Methods of Bitumen and Bituminous Mixtures for Highway Engineering (JTG E20-2011) are shown in Table 1. Limestone (10–20, 5–10 and 0–5 mm) is used as coarse aggregate in the test. And fine aggregate in HMA is finely ground limestone powder. The physical properties of coarse aggregate and fine aggregate are presented in Tables 2 and 3, respectively. The gradation of HMA is in the range of AC-20 (i.e. the maximum nominal aggregate size of asphalt concrete is 20 mm, referring to the Chinese Specifications for Design of Highway Asphalt Pavement (JTG D50-2006)), as shown in Figure 1.

According to AASHTO T-312, the gyratory compaction method was used to prepare HMA mixture slab. Then, core sampling was done to obtain cylindrical specimens (with the height of 150 ± 2 mm, diameter of 100 ± 2 mm).

Table 1. Property indexes of SBS-modified asphalt.

Index	Test results
Density at 15°C (g/cm^3)	1.035
Penetration at 25°C, 100 g, 5 s (0.1 mm)	57
Ductility at 5°C, 5 cm/min (cm)	35
Softening point *T* (°C)	80
Flash point (°C)	348
Solubility (%)	99.72
Viscosity at 135°C (Pa·s)	1.8
RTFO test	
Mass loss (%)	0.02
Penetration ratio (%)	80
Ductility at 5°C (cm)	22
Grade	PG 76-28

Table 2. Technical parameters of coarse aggregate.

Parameter	Test results
Crushing value (%)	12.5
Los Angeles abrasion loss (%)	14.5
Adhesiveness of asphalt (°)	5.0
Ratio of needle and plate grain (%)	4.3
Soft rock content (%)	0.4

Table 3. Technical parameters of fine aggregate.

Parameter	Test results
Sand equivalent (%)	82.8
Methylene blue value (g/kg)	2.0
Angularity (flow time) (s)	39.0

3. Making and characterisation of mechanical damage

3.1 *Damage making*

In order to compare the effect of damage-making method on damage, two loading methods were employed to make mechanical damage of specimens. One was the monotonous uniaxial compression loading using the universal

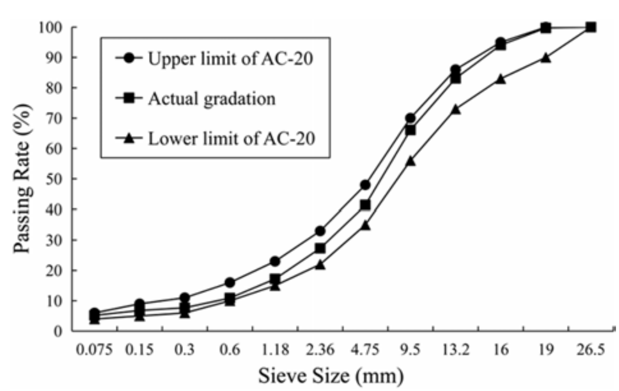

Figure 1. Grading curve of aggregates.

testing machine (UTM-100), and the other was the repetitive compression loading using a universal servo-controlled load system (MTS810).

3.1.1 *Monotonous compression loading*

Referring to bituminous mixture uniaxial compression test (JTG E20-2011), the prepared specimens were compressed with the loading rate of 2 mm/min at the ambient temperature of 25°C. When the amounts of compression of specimens separately attained to 2, 4, 6 and 7 mm, the loads were unloaded and then the permanent deformations of specimens were measured. Different permanent deformations reflected different damage states. For each damage state, three damaged specimens were prepared for the following permeability tests and HWTD tests.

3.1.2 *Repetitive compression loading*

Repetitive haversine load pulses of 0.1-s duration followed by a rest period of 0.9 s were applied on specimens at the ambient temperature of 25°C. The dynamic stress peak was 0.4 MPa. When the cumulative compression amounts of specimens separately attained to 2, 4, 6 and 7 mm, the cyclic loading was stopped and then the permanent deformations of specimens were measured.

3.2 *Characterisation of damage*

Two kinds of nondestructive testing methods were employed to characterise the mechanical damage of HMA: dynamic modulus testing method and ultrasonic wave testing method.

3.2.1 *Dynamic modulus testing method*

Asphalt pavement suffers a dynamic process of repeated loading and unloading under the traffic loads. So dynamic modulus of HMA was used to characterise damage.

In this study, the dynamic modulus of HMA was obtained by the simple performance test (SPT). The dynamic modulus test is a nondestructive testing method based on the standard test for dynamic modulus of asphalt mixture (ASTM D3497). The specimens used in SPT were required to be the standard size (150 ± 2 mm high). In test, a continuous sinusoidal load was employed to apply on the cylindrical specimen:

$$\sigma(t) = \sigma_0 \sin 2\pi f t, \tag{1}$$

where σ_0 is the stress peak; f is the loading frequency, and f is taken as 10 Hz in this study, according to the investigation done by Huang (1993).

The damage of HMA can be expressed as follows:

$$D = 1 - \frac{|\tilde{E}^*|}{|E^*|}, \tag{2}$$

where D is damage; $|E^*|$ is the dynamic modulus of undamaged HMA; $|\tilde{E}^*|$ is the dynamic modulus of damaged HMA.

Due to the viscosity property of HMA, the strain response lags behind the periodic stress by a phase angle. The dynamic modulus in Equation (2) is the ratio of maximum stress to maximum strain, and so it is a complex modulus.

Figure 2 shows the relationship between damage and permanent deformation of HMA. It can be seen that the damage first slowly increases with permanent deformation, then quickly develops. When the deformation rises to about 4%, the increasing rate of damage gradually gets slow. The damages made by the monotonous and repetitive loading methods have little distinction. This indicates that the repetitive loading method can be replaced by the monotonous loading method to make the mechanical damage of HMA. In the following permeability tests and HWTD tests, only the monotonous loading method was used to make damage.

It can be found from Figure 2 that even a small permanent deformation can cause mechanical damage. This is because at the ambient temperature of 25°C, the asphalt is quasi-fragile material and small deformation can lead to the initiation of microcracks, as shown in Figure 3.

Variations of damages from the two making methods with the permanent deformation can be well fitted with the Gaussian function:

$$D = -0.081 + 0.636\mathrm{e}^{-(\varepsilon_p - 4.803)^2/16.524} \quad (R^2 = 0.980), \tag{3}$$

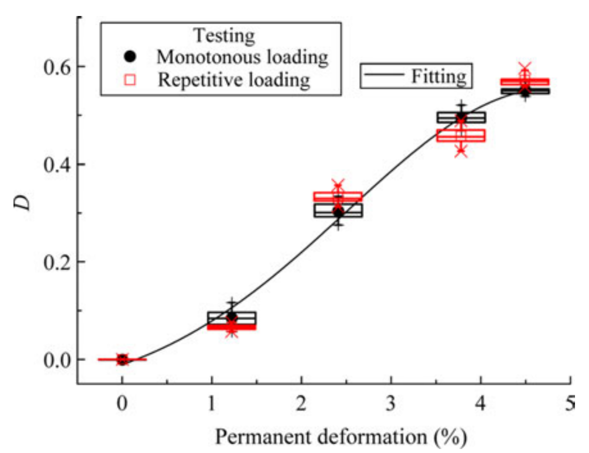

Figure 2. Variation of mechanical damage with permanent deformation of HMA.

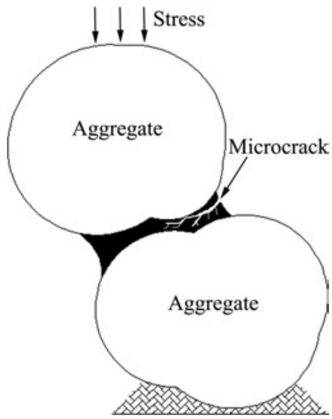

Figure 3. Sketch of initiation of microcracks.

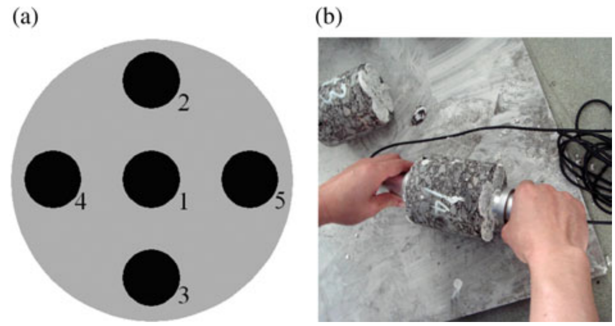

Figure 4. Ultrasonic wave velocity test: (a) arrangement of measuring points and (b) test photograph.

where ε_p is the permanent deformation; R^2 is the square of correlation coefficient, which implies the fitting precision.

3.2.2 *Ultrasonic wave testing method*

In recent years, the ultrasonic testing technique is used in practical engineering, such as evaluating the performance of HMA (Yi *et al.* 2009) and controlling the construction quality of asphalt pavement (Birgisson *et al.* 2003). These tentative applications have achieved satisfactory results. In this study, the ultrasonic testing technique is utilised to characterise HMA damage. Compared with the dynamic modulus testing method in SPT, the ultrasonic wave method has a better adaptation to specimen size.

Supposing the ultrasonic wave propagation in specimens is one-dimensional, according to the wave theory, the damage characterised by the ultrasonic wave velocity (Wang 1985) can be expressed as follows:

$$D_u = 1 - \frac{\tilde{V}^2}{\bar{V}^2}, \tag{4}$$

where $\bar{V}$ and $\tilde{V}$ are the ultrasonic wave velocities of the undamaged and damaged material, respectively.

At the ambient temperature of 25°C, the ultrasonic wave velocities of eight groups of SPT standard specimens (100 ± 2 mm in diameter, 150 ± 2 mm high) were tested with the nonmetal ultrasonic detector to obtain $\bar{V}$ and $\tilde{V}$ before and after damaged. Before tests, the specimens were dried with the blower to avoid the effect of moisture on ultrasonic wave velocity. To ensure good contact between the probes and the end faces of the specimen, putty plaster was used as the coupling medium. Compared with conventional coupling materials such as vaseline, the putty plaster is easy to wash away after the test to avoid influencing the permeability of the specimen in the following permeability test. The ultrasonic wave velocities corresponding to the five measuring points marked in Figure 4 were tested, and the average value was taken as the ultrasonic wave velocity of the specimen.

Figure 5 shows the relationship between the damage D characterised by the dynamic modulus (Equation (2)) and the damage D_u characterised by the ultrasonic wave velocity (Equation (4)). At the ambient temperature of 25°C, the relation between D and D_u can be expressed as:

$$D = 4.435 D_u^{1.564} \quad (R^2 = 0.994). \tag{5}$$

Obtaining D_u, D can be known according to Equation (5). For the same HMA standard specimen, D is not equal to D_u. This is mainly because the ultrasonic detector probe diameter (37 mm) is less than the specimen diameter (100 mm), and this makes the ultrasonic wave propagate in the specimen more than one-dimensional, which does not agree with the assumption of Equation (4).

The specimens used in the following permeability test and HWTD test were not the standard specimens of SPT (150 ± 2 mm high). But Equation (5) is only appropriate for the standard specimen of SPT. Considering the effect of specimen size on the D–D_u correlation, Equation (5) needs to be modified. Therefore, the ultrasonic wave

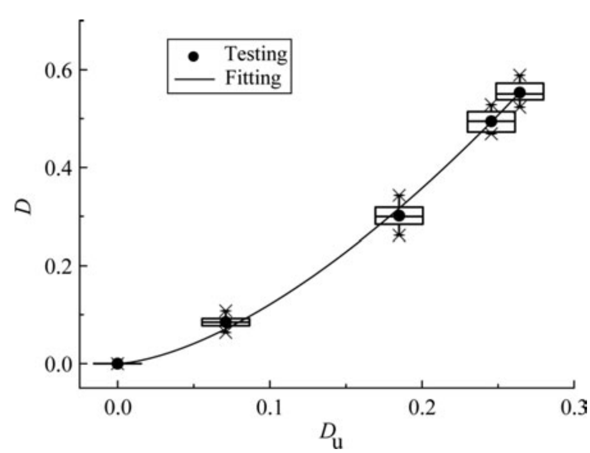

Figure 5. Relationship between D and D_u.

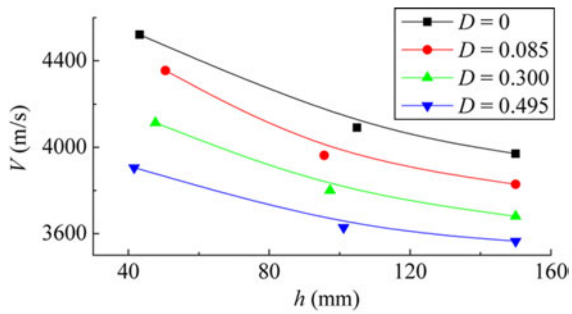

Figure 6. Relationship between V and h.

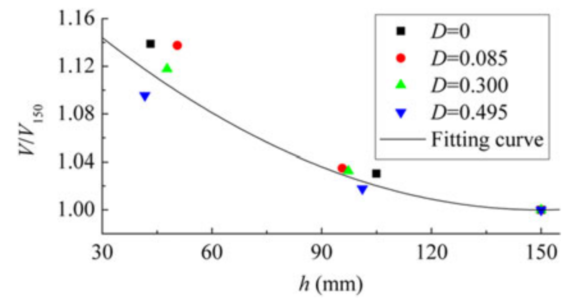

Figure 7. Relationship between V/V_{150} and h.

velocities of the specimens with different damage states and heights were measured. The detailed processes were: first, four groups of standard specimens were monotonously compressed with the UTM testing machine to obtain different permanent deformations, and then the dynamic modulus method was used to measure the damages D; second, the ultrasonic wave method was used to measure the damages D_u of damaged standard specimens; Finally, each specimen is transversely cut into two fractions at about one-third of the height, and then ultrasonic wave tests were conducted for each fraction.

Figure 6 shows the variations of ultrasonic wave velocity V with the specimen height h and damage D. It can be seen that the ultrasonic wave velocity nonlinearly decreases with the increase of specimen height. And for different damages, V–h curve patterns are basically similar. For specimens with the same damage, the normalised wave velocity V/V_{150} can be obtained by dividing the wave velocity V with the wave velocity V_{150} of the standard specimen (150 ± 2 mm high), as shown in Figure 7. Figure 7 shows the relationship between normalised wave velocity V/V_{150} and the specimen height h has little relevance with the damage. Therefore, for different damages, V/V_{150}–h curve can be fitted with the following single function:

$$\frac{V}{V_{150}} = 1 + 0.225\left(\frac{h}{150} - 1\right)^2, \tag{6}$$

where h is the specimen height in mm.

Equation (6) can be further expressed as:

$$V_{150} = \frac{V}{[1 + 0.225((h/150) - 1)^2]}. \tag{7}$$

In Equation (4), D_u is obtained based upon the standard specimen of 150 mm height. In order to express more clearly, Equation (4) is rewritten as:

$$D_u = 1 - \frac{\tilde{V}_{150}^2}{\bar{V}_{150}^2}, \tag{8}$$

where $\bar{V}_{150}$ and $\tilde{V}_{150}$ are the ultrasonic wave velocities of the undamaged and damaged standard specimen, respectively.

According to Equation (7), the relationships of ultrasonic wave velocity between standard and nonstandard specimens before and after damage can be got, respectively, as follows:

$$\bar{V}_{150} = \frac{\bar{V}}{[1 + 0.225((\bar{h}/150) - 1)^2]}, \tag{9}$$

$$\tilde{V}_{150} = \frac{\tilde{V}}{[1 + 0.225((\tilde{h}/150) - 1)^2]}, \tag{10}$$

where $\bar{h}$ and $\tilde{h}$ are the height of undamaged and damaged specimens, respectively.

Substituting Equations (9) and (10) into Equation (8) can obtain the following damage expression of nonstandard specimen-based ultrasonic wave velocity:

$$D_u = 1 - \frac{\tilde{V}^2[1 + 0.225((\bar{h}/150) - 1)]^2}{\bar{V}^2[1 + 0.225((\tilde{h}/150) - 1)^2]^2}. \tag{11}$$

If $\bar{h} = \tilde{h}$, the Equation (11) can be simplified to Equation (4). This illustrates that whatever the height of the specimen is, if the height of damaged specimen is equal to that of the undamaged specimen, Equation (11) has the same expression with Equation (4). So in this case, D_u needs no modification. However, if the heights of undamaged and damaged specimens are not equal, the D_u should be modified by Equation (11). Taking Equation (11) into Equation (5), the damage D characterised by dynamic modulus can be obtained. In the following permeability tests and HWTD tests, Equation (11) was used to convert the D_u of the nonstandard specimen to D of the standard specimen.

4. Effect of mechanical damage on permeability of HMA

Permeability of HMA plays an important role in the evolution of moisture damage of pavement. In this study,

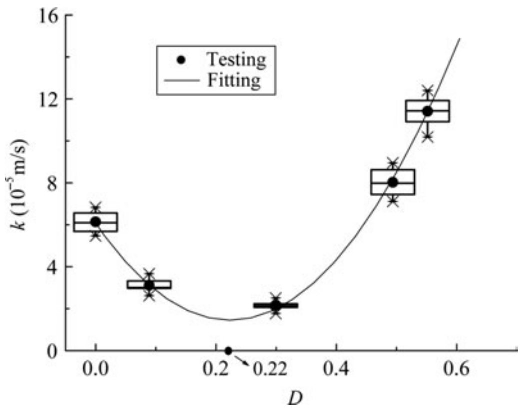

Figure 8. Relationship between permeability coefficient and damage.

the effect of the mechanical damage on HMA permeability was investigated.

The Karol-Warner permeameter was used to test the coefficient of permeability, following the Florida DOT permeability testing method (FM 5-565). The permeability tests were conducted at the ambient temperature of 25°C. Before tests, specimens were uniaxially compressed with the monotonous loading method to make different mechanical damages. Because the specimens (60 mm high) were not the standard specimens of SPT, damages first were measured with the ultrasonic wave method and then were converted to the damages characterised by dynamic modulus with Equation (5).

Figure 8 shows the variation curve of permeability coefficient with damage. The permeability does not monotonously increase with the increase of the damage, but first decreases and then increases. This is because when damage is small, and the air voids are slightly compressed along with the initiation of microcracks. When damage develops to a certain level, the macrocracks rapidly propagate and coalesce, and this makes the permeability of HMA increase with the increase of damage. As shown in Figure 8, the permeability–damage curve has a damage threshold $D_{cr} = 0.22$. When D is more than 0.22, the permeability quickly increases with damage, and so water can easily infiltrate into pavement and speeds up the moisture damage in asphalt pavement.

The relation curve of the permeability and damage shown in Figure 8 can be well fitted with the following equation:

$$k = 6.059 - 41.213D + 92.207D^2 \quad (R^2 = 0.998), \quad (12)$$

where k is the permeability coefficient in 10^{-5} m/s.

5. Effect of mechanical damage on moisture damage

HWTD test was performed to study the effect of mechanical damage on the evolution of moisture damage.

Figure 9. Assembly of specimen in HWTD test.

Compared with the traditional wheel tracking testers, the HWTD is the more rigorous device to evaluate and predict moisture damage of HMA because of using steel wheels rather than rubber wheels. Two stainless steel wheels have a diameter of 203 mm and a width of 47 mm. The wheel load is fixed at 685 N and the average contact stress is 0.73 MPa approximating the stress produced by one rear tire of a double-axle truck. A match face on each of the two prepared specimens (60 mm in height and 150 mm in diameter) was cut so as the radius square to the face is 60 ± 1 mm. The cut specimens were assembled in high density poly-ethylene forms as shown in Figure 9.

The variation curve of the rut depth with the number of wheel passes can be obtained from HWTD test, as shown in Figure 10. The creep slope is the inverse of the deformation rate within the linear region of the deformation curve prior to stripping (if stripping occurs) and measures the rutting susceptibility. The stripping slope is the inverse of the deformation rate within the linear deformation of the deformation curve, after the stripping began. The striping inflection point and the stripping slope are used to measure moisture damage. The stripping

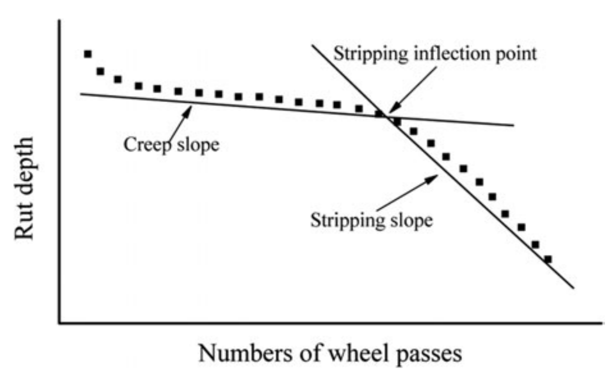

Figure 10. Typical HWTD test curve.

Table 4. HWTD test cases.

	Mechanical damage		Water temperature (°C)
Case	Initial damage D_0	Developing damage	
1	0	No	25
2	0.26	No	25
3	0.46	No	25
4	0	No	60
5	0.26	No	60
6	0.46	No	60
7	0	Yes	25
8	0	Yes	60

inflection point is the number of wheel passes corresponding to the intersection of the creep slope and the stripping slope. The stripping slope measures the accumulation of permanent deformation primarily due to moisture damage and is used to estimate the relative resistance of the HMA to moisture damage. The lower the inverse stripping slope, the more severe the moisture damage (Aschenbrener 1995).

5.1 *Testing program*

HWTD test cases are shown in Table 4. Two types of mechanical damage were introduced: initial damage and developing damage.

For the initial damage cases, specimens were uniaxially compressed with the monotonous loading method to make different mechanical damages before tests. Initial damages first were measured with the ultrasonic wave method and then were converted to the damages characterised by dynamic modulus. Specimens with different initial damages of 0, 0.26 and 0.46 were tested.

For the developing damage cases, specimens were not damaged initially, but mechanical damages can significantly vary during tests. In order to induce the developing damage, two layers of rubber cushions (Figure 11) with 10 mm thick were stacked under the specimens in HWTD tests (correspondingly, the height of the HWTD test specimen was reduced from 60 to 40 mm). The shore hardness of rubber material was 65°, the tensile strength was 6 MPa and the elongation was 202%. To predict the influence of rubber cushions on the stress states in specimens, the ANSYS finite element program was employed to numerically simulate the stress states in specimens under wheel load in HWTD test. Figure 12 shows the contour of the horizontal normal stress perpendicular to the travel direction at the bottom of specimen (note that the tension is positive). It can be seen that for the test case with rubber cushions, the maximum tensile stress is 0.11 MPa and is 4.5 times larger than that in the test case without rubber cushions. It is implied that the mechanical damage is susceptible to be induced after

Figure 11. Rubber cushions.

adding rubber cushions. The developing damage can reflect the effect of undesirable stress states such as tensile stress state induced by poor interlayer bonding or internal defect in the pavement. The undesirable stress state can speed up the generation and evolution of the mechanical damage, which causes the increase of the permeability of pavement and accelerates the moisture damage.

In addition, a large number of investigations on pavement distresses discovered that the moisture damage was more likely to occur in a hot and humid environment (Al-Swailmi and Terrel 1992, Terrel and Al-swailmi 1994, Little and Jones 2003, Arambula *et al.* 2007, Bausano and Williams 2009, Cho and Bahia 2010, Huang *et al.* 2010). So this study considered the effect of the water temperature on moisture damage in pavement. In HWTD tests, the ambient temperatures of 25 and 60°C were used, as shown in Table 4.

5.2 *Test results and analyses*

In this study, the cumulative deformation of specimen was introduced to analyse the test results:

$$\varepsilon_c = \varepsilon_0 + \frac{s}{h}, \tag{13}$$

where ε_c is the cumulative deformation; ε_0 is the initial deformation corresponding to the initial damage of specimen; s is the average rut depth; h is the specimen height.

The cumulative deformation is the sum of the initial deformation and the newly emerged deformation during the test. Figures 13 and 14 show the effects of the initial and developing mechanical damages on the evolution curves of the cumulative deformation, respectively.

5.2.1 *Effect of initial mechanical damage on moisture damage*

Figure 13 shows the effect of the initial mechanical damages on the evolution curves of the cumulative

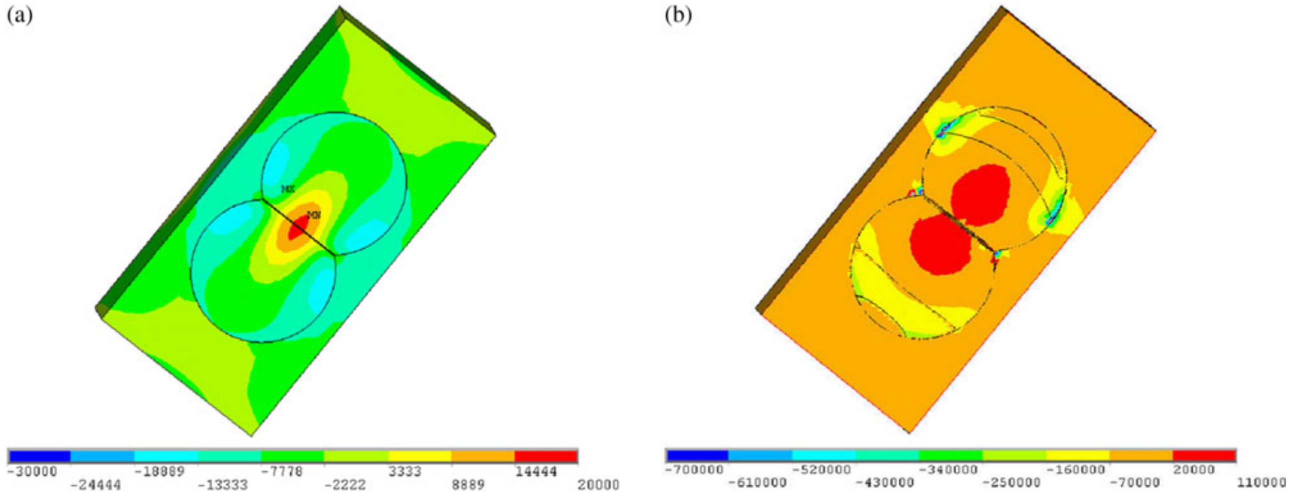

Figure 12. Stress contours at the bottom of specimens (unit: kPa): (a) without rubber cushions and (b) with rubber cushions.

deformation. It can be seen from Figure 13(a) that regardless of the initial mechanical damages of specimens, at the water temperature of 25°C, the striping inflection points do not appear on cumulative deformation curves until the number of wheel passes attains 40,000. But at the water temperature of 60°C, stripping inflection points appear before the number of wheel passes attain 20,000, as shown in Figure 13(b). This demonstrates that the pavements in hot and humid environment are easier to suffer moisture damage. This is because with the increase of water temperature, the adhesion and cohesion of asphalt reduce. Under the dynamic stresses and scouring forces in pavement induced by the repeated wheel loads, asphalt membrane is easily damaged and rushed out of pavement. The asphalt mixture loses strength to become ravelling, and finally potholes occur on the pavement.

It can be seen from Figure 13 that the initial mechanical damage has an important influence on the cumulative deformation. When the water temperature is 25°C, the larger initial damage can cause larger cumulative deformation. However, when the water temperature is 60°C, the effect of the initial damage on the cumulative deformation is different, and it can be summarised as follows: Before the stripping inflection point appears, the cumulative deformation increases with the increase of initial mechanical damage; but after the stripping inflection point, when the initial mechanical damage $D_0 = 0$, the cumulative deformation is maximum, and when $D_0 = 0.26$, the cumulative deformation is minimum. It is implied that at the water temperature of 60°C, the effect of the initial damage on the evolution of moisture damage is nonlinear. This may be because of the specimens with different initial damage, their initial permeability coefficients are different. The permeability coefficient is maximum when $D_0 = 0$, and is minimum when $D_0 = 0.26$, as shown in Figure 8. The changed permeability induced by mechanical damage plays an important role in the evolution of moisture damage.

5.2.2 *Effect of developing mechanical damage on moisture damage*

Figure 14 shows the effect of the developing mechanical damages on the evolution curves of the cumulative

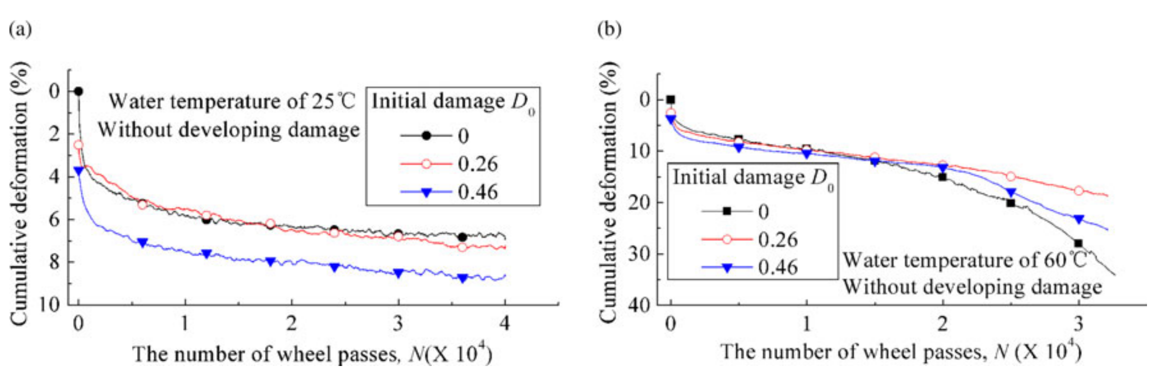

Figure 13. Effect of initial damage on cumulative settlement: (a) water temperature of 25°C and (b) water temperature of 60°C.

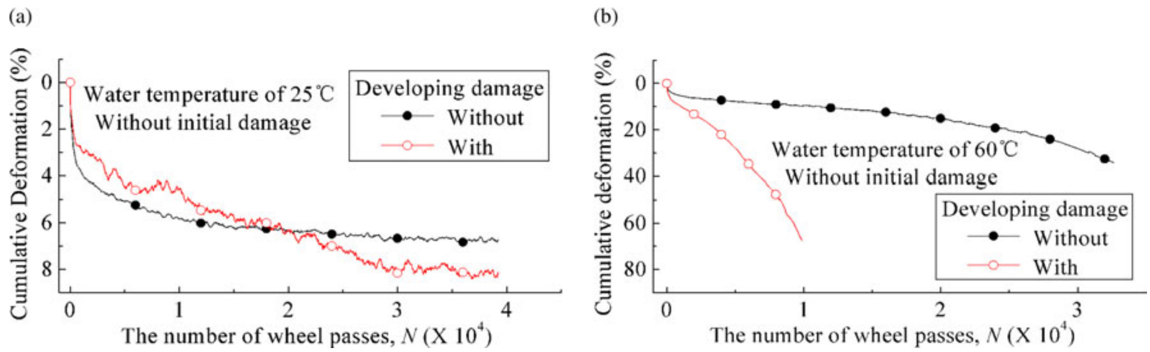

Figure 14. Effect of developing damage on cumulative deformation: (a) water temperature of 25°C and (b) water temperature of 60°C.

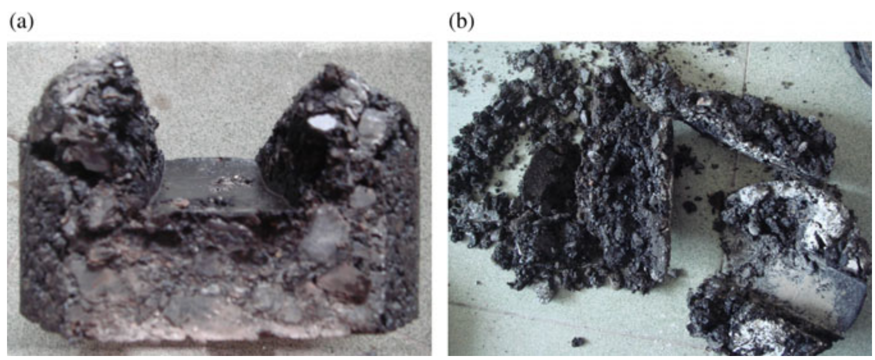

Figure 15. Photographs of specimens after tests at the water temperature of 60°C: (a) without developing damage and (b) with developing damage.

deformation. It can be seen that the developing mechanical damage has an important influence on the cumulative deformation. For the test cases with developing damage, the cumulative deformations are larger than that in the test cases without developing damage. Moreover, the influences of the developing mechanical damage on the evolution of moisture damage have a strong dependence on water temperature. When the water temperature is 25°C, the striping inflection points do not appear (Figure 14(a)). However, when the water temperature is 60°C, the striping point appears. Compared with the test case without developing damage, it is much earlier that the striping inflection point appears with developing damage. This is because with the higher environment temperature, the HMA gets weaker. When the water temperature is 60°C, compared with the water temperature of 25°C, the undesirable stress (tensile stress) in the specimen is closer to the fatigue failure strength and can induce more serious damage (like cracking). The induced damage increases the permeability of HMA. Meanwhile, the adhesion and cohesion of asphalt get weaker with higher environment temperature. Consequently, comprehensive factors can aggravate the moisture damage of the pavement.

Figure 15 shows the photographs of specimens after tests at the water temperature of 60°C. It can be seen that the failure of the specimen with the developing damage is more serious than that without the developing damage. With the developing damage, specimen got completely ravelling when the number of wheel passes attains 10,000, as shown in Figure 15(b). This demonstrates the above analyses for the effect of developing mechanical damage on moisture damage. Therefore, preventing undesirable stress states in pavement is a significant approach to reducing risk of moisture damage.

6. Conclusions

In this study, the permeability tests and the HWTD tests were carried out to tentatively study the effect of traffic-load-induced mechanical damage on the evolution of moisture damage in HMA pavement. The tested pavement material was the SBS-modified HMA. The mechanical damages of specimens were artificially made with the monotonous uniaxial compression loading method and the repetitive compression loading method, respectively. Two kinds of nondestructive testing methods, that is the dynamic modulus testing method and the ultrasonic wave testing method, were employed to characterise the damages. The investigation leads to the following conclusions:

(1) The damages made with the two kinds of damage making methods have little difference. So the repetitive compression loading method can be replaced by the monotonous compression loading method. The mechanical damage increases with the increase of permanent deformation, and even small permanent deformation also induces mechanical damage. The damages characterised with the dynamic modulus method and the ultrasonic wave method can be converted each other by an empirical function.

(2) The HMA permeability presents a parabolic relationship with the damage. The permeability coefficient initially decreases and then increases with the increase of damage.

(3) The mechanical damage has a significant influence on the moisture damage, especially in hot and humid environment. In HWTD test, the mechanical damage induced by the undesirable stress state in pavement accelerates the appearance of the striping inflection point and increases the cumulative deformation of HMA specimen. Therefore, in order to reflect the performance of asphalt pavement during its life cycle, the effect of mechanical damage on the evolution of moisture damage should be considered in pavement design and construction.

Funding

This work was supported by the Chinese Natural Science Foundations [grant number 51279094], [grant number 51078222], [grant number 50708056], the Natural Science Foundations of Shandong Province, China [grant number ZR2011EEM012], Independent Innovation Foundation of Shandong University (IIFSDU) [grant number 2012HW003] and the Program for New Century Excellent Talents in University of Ministry of Education of China [grant number NCET-13-0340].

References

Airey, G.D., *et al.*, 2008. The influence of aggregate, filler and bitumen on asphalt mixture moisture damage. *Construction and Building Materials*, 22 (9), 2015–2024.

Al-Swailmi, S. and Terrel, R.L., 1992. Evaluation of water damage of asphalt concrete mixtures using the environmental conditioning system (ECS). *Journal of Association of Asphalt Paving Technologists*, 61, 405–445.

Arambula, E., Masad, E., and Martin, A.E., 2007. Influence of air void distribution on the moisture susceptibility of asphalt mixes. *Journal of Materials in Civil Engineering*, 19 (8), 655–656.

Aschenbrener, T., 1995. Evaluation of Hamburg wheel-tracking device to predict moisture damage in hot-mix asphalt. *Transportation Research Record*, 1492, 193–201.

Bausano, J. and Williams, R.C., 2009. Transitioning from AASHTO T283 to the simple performance test using moisture conditioning. *Journal of Materials in Civil Engineering*, 21 (2), 73–74.

Birgisson, B., Roque, R., and Page, G.C., 2003. Ultrasonic pulse wave velocity test for monitoring changes in hot-mix asphalt mixture integrity from exposure to moisture. *Transportation Research Record*, 1832, 173–181.

Brown, E.R., 1990. Density of asphalt concrete how much is needed? *Transportation Research Record*, 1282, 27–32.

Buchanan, M.S. and Moore, V.M., 2005. *Laboratory accelerated stripping simulator for hot mix asphalt*. Starkville, MS: Monograph Mississippi Transportation Research Center, James Worth Bagley College of Engineering, Mississippi State University.

Cheng, D., *et al.*, 2002. Use of surface free energy properties of the asphalt–aggregate system to predict moisture damage potential. *Journal of Association of Asphalt Paving Technologists*, 71, 59–88.

Cho, D.W. and Bahia, H.U., 2010. New parameter to evaluate moisture damage of asphalt–aggregate bond in using dynamic. *Journal of Materials in Civil Engineering*, 22 (3), 267–268.

Cui, X.Z., 2010. Dynamic numerical analysis of anti-moisture-damage mechanism of permeable pavement base. *International Journal of Geomechanics–ASCE*, 10 (6), 230–235.

Delaporte, B., *et al.*, 2008. Effect of ultrafine particles on linear viscoelastic properties of mastics and asphalt concretes. *Transportation Research Record: Journal of the Transportation Research Board*, 2051, 41–48.

Guo, X., *et al.*, 2011. The research of bituminous mixture water stability based on aggregate cleanness. *Advanced Materials Research*, 255–260, 3297–3301.

Hicks, R.G., *et al.*, 2003. Road map for mitigating national moisture sensitivity concern in hot mix pavements. *In*: *Moisture sensitivity of asphalt pavements – A national seminar*, 4–6 February 2003, San Diego, CA, USA. Washington, DC: Transportation Research Board, 331–341.

Huang, Y.H., 1993. *Pavement analysis and design*. Delhi: Pearson Education.

Huang, B.S., Shu, X., and Dong, Q., 2010. Laboratory evaluation of moisture susceptibility of hot-mix asphalt containing cementitious fillers. *Journal of Materials in Civil Engineering*, 22 (7), 666–668.

Kanitpong, K. and Bahia, H., 2005. Relating adhesion and cohesion of asphalt to the effect of moisture on laboratory performance of asphalt mixtures. *Transportation Research Record: Journal of the Transportation Research Board*, 1901, 33–43.

Kanitpong, K. and Pummarin, K., 2010. Investigation of industrial wastes in hot mix asphalt for moisture damage resistance. *Journal of Solid Waste Technology and Management*, 36 (2), 81–90.

Kiggundu, B.M. and Roberts, F.L., 1988. *The success/failure of methods used to predict the stripping potential in the performance of bituminous pavement mixtures*. Auburn, AL: National Center for Asphalt Technology Report 88–92.

Kringos, N. and Scarpas, A., 2008. Physical and mechanical moisture susceptibility of asphaltic mixture. *International Journal of Solids and Structures*, 45, 2671–2685.

Krishnan, J.M. and Bao, C.L., 2001. Permeability and bleeding of asphalt concrete using mixture theory. *International Journal of Engineering Science*, 39 (6), 611–627.

Little, D.N. and Jones, D.R., 2003. Chemical and mechanical processes of moisture damage in hot-mix asphalt pavements. *In*: *Moisture sensitivity of asphalt pavements – A national seminar*, 4–6 February 2003, San Diego, CA, USA. Washington, DC: Transportation Research Board, 37–70.

Masad, E., Castelblanco, A., and Birgisson, B., 2006. Effects of air void size distribution, pore pressure, and bond energy on moisture damage. *Journal of Testing and Evaluation*, 34 (1), 9–16.

Mohammad, L.N., *et al.*, 2000. Mechanistic evaluation of hydrated lime in hot mix bitumen mixtures in transportation. *Transportation Research Record: Journal of the Transportation Research Board*, no. 1723, 26–36.

Solaimanian, M., Kennedy, T.W., and Elmore, W.E., 1993. *Long-term evaluation of stripping and moisture damage in asphalt pavements treated with lime and anti-stripping agents*. Austin, TX: Center for Transportation Research, University of Texas at Austin, Report 1286-1F.

Taylor, M.A. and Khosla, N.P., 1983. Stripping of asphalt pavements: state of the Art. *Transportation Research Record*, 911, 150–158.

Terrel, R.L. and Al-Swailini, S., 1993. The role of pessimum voids concepts in understanding moisture damage to asphalt concrete mixtures. *Transportation Research Record*, 1386, 31–37.

Terrel, R.L. and Al-Swailmi, S., 1994. *Water sensitivity of asphalt-aggregate mixes: test selection*. Washington, DC: Strategic Highway Research Program, National Research Council, SHRP Report A-403.

Wang, L.L., 1985. *Foundation of stress waves*. Beijing: National Defence Industry Press.

Yuan, Y.Q., *et al.*, 2011. Experimental study on water stability of asphalt mixture. *Advanced Materials Research*, 266, 135–138.

Yi, Y.J., *et al.*, 2009. Application of ultrasonic test method in freeze-thaw test of asphalt mixture. *Journal of Highway and Transportation Research and Development*, 26 (11), 6–10.